Journal of Alloys and Compounds 509 (2011) 2650–2653

Contents lists available at ScienceDirect

Journal of Alloys and Compounds

journal homepage: www.elsevier.com/locate/jallcom

Synthesis and hydriding behavior of Li_2MgPt

J.R. Salvador*, J.F. Herbst, M.S. Meyer

Chemical Sciences and Materials Systems Laboratory, General Motors Research and Development Center, Mail Code 480-106-224, Warren, MI 48090-9055, United States

ARTICLE INFO

Article history:
Received 8 November 2010
Accepted 24 November 2010
Available online 3 December 2010

Keywords:
Hydrogen absorbing materials
Metal hydrides
Electronic band structure
Enthalpy

ABSTRACT

We describe preparation of the ternary intermetallic Li_2MgPt and determination of its crystal structure and hydrogen sorption behavior. Phase formation was suggested by density functional theory calculations. The compound crystallizes in the cubic $P\bar{4}3m$ space group and is isostructural to Li_2MgSi and Li_2MgIr. Its reaction with hydrogen proceeds according to $Li_2MgPt + H_2 \rightarrow MgPt + 2LiH$, in which MgPt is a new member of the Mg–Pt binary phase diagram.

1. Introduction

Li_2MgX ternary compounds are known to form for X = Ag, Al, Au, Bi, Cd, Ga, Ge, Hg, In, Pb, Sb, Si, Sn, Tl, and Zn in various face-centered cubic (fcc) space groups [1]. Since these phases contain substantial amounts of the light elements Li and Mg, this class of materials merits exploration as potential hydrogen storage media. We have estimated enthalpies of formation ΔH via density functional theory (DFT [2]) using two of the established structures as templates [Li_2MgPb-type ($Fm\bar{3}m$; No. 225) and $CuHg_2Ti$-type ($F\bar{4}3m$; space group No. 216)], finding negative values indicating phase formation for the known compounds as well as for other elements X, among them Ir and Pt. Preparation of Li_2MgIr and the quaternary hydride $LiMgIrH_6$, also previously unknown, was documented previously [3]. Here we report synthesis of Li_2MgPt and determination of its crystal structure. Exposure to hydrogen produces LiH and MgPt, which we identify as a new Mg–Pt binary compound.

2. Experimental and calculational procedures

Li_2MgPt was synthesized by mechanical alloying. In the optimal preparation route Li pieces (Averton, 99.9%), Mg powder (Alfa Aesar, 99.9% ~325 mesh), and Pt powder (Alfa Aesar, 99.99% ~325 mesh) were combined in 2:1.5:1 Li:Mg:Pt atomic ratios that were found to minimize the formation of secondary phases as well as to compensate for Mg loss due to plating on the milling vial walls. All sample manipulation was done in an Ar-filled glove box with O_2 and H_2O levels of 2–3 ppm or below. The materials were dry milled under Ar in a SPEX Certiprep 8000 high energy mill for 5 h. Elemental analysis by inductively coupled plasma mass spectrometry performed on product from the optimized milling reaction with excess Mg indicated Li:Mg:Pt ratios of 2:1.07:1, very near the target stoichiometry.

Hydriding of Li_2MgPt was performed in a Cahn TG-2151 high-pressure thermogravimetric analyzer (hTGA) by heating under a hydrogen atmosphere of 82 bar at a rate of 5 °C/min to a final temperature of approximately 400 °C and then holding for 700 min. Thermal desorption measurements to monitor mass loss were conducted in 1.3 bar helium, and a SRS CIS 100 mass spectrometer was used to analyze the desorbed species.

For structural analysis sample powder was loaded into a 1.0 mm quartz capillary and powder X-ray diffraction (PXRD) data collected on a STOE II imaging plate diffractometer in transmission geometry at room temperature with graphite monochromatized Mo Kα radiation. Data were obtained between 5° and 70° 2θ and integrated over the surface of the plate not shadowed by the capillary. The final structure was refined by least squares Rietveld analysis using the FULLPROF suite of programs [4].

Total electronic energies were computed with the Vienna *ab initio* Simulation Package (VASP), which implements DFT with a plane wave basis set [5,6]. Potentials obtained via the projector-augmented wave approach [7,8] were employed for the elements in conjunction with the generalized gradient approximation of Perdew and Wang [9,10] for the exchange-correlation energy functional. The Li, Mg, Pt, and H potentials contained 3, 8, 10, and 1 valence electrons and were constructed with plane wave energy cutoffs of 272 eV, 266 eV, 230 eV, and 700 eV, respectively. In all self-consistent calculations a plane wave cutoff energy of at least 900 eV, much larger than any of the potential cutoffs, was imposed. The k-point spacings of the reciprocal space meshes were no larger than 0.1 $Å^{-1}$. At least two full-cell optimizations of the lattice constants and nuclear coordinates were performed for each material of interest; the total energies were converged to 10^{-6} eV/cell and the forces relaxed to 10^{-4} eV/Å.

3. Li_2MgPt characterization

We determined the crystal structure of Li_2MgPt by Rietveld analysis on both an as-milled sample and a second sample obtained by thermal desorption of a hydrided specimen. As was the case for the Li_2MgIr [3] and Li_2MgSi [11] analogs investigated previously, a low angle peak in each of the PXRD patterns was found to be inconsistent with the fcc templates employed in the exploratory DFT work. The structure was refined successfully within the

* Corresponding author. Tel.: +1 586 986 5383; fax: +1 586 986 3091.
E-mail address: james.salvador@gm.com (J.R. Salvador).

0925-8388/$ – see front matter © 2010 Elsevier B.V. All rights reserved.
doi:10.1016/j.jallcom.2010.11.180

Table 1
Crystallographic information for Li_2MgPt obtained for an as-milled sample, a hydrogen-cycled sample, and from DFT optimization of the structure. Li_2MgPt forms in the primitive cubic $P\bar{4}3m$ space group (No. 215) and has four formula units per unit cell. The Li, Mg, and Pt ions reside on (1b, 3c, 4e), (1a, 3d), and 4e sites, respectively. R_{wp} is the weighted profile quality-of-fit index for the Rietveld refinement.

Li_2MgPt			
	As-milled	Cycled	DFT
a (Å)	6.289(1)	6.295(1)	6.292
Li 4e x	0.7270	0.7270	0.7262
Pt 4e x	0.2458	0.2449	0.2501
V (Å^3)	248.7	249.4	249.1
ρ (g/cm^3)	6.23	6.21	6.220
R_{wp} (%)	12.4	13.0	

$$R_{wp} = \frac{\sum \left| w_i(y_i(obs) - y_i(obs))^2 \right|^{\frac{1}{2}}}{\sum |w_i(y_i(obs))|^2}.$$

non-isomorphic sub-group, $P\bar{4}3m$, of the $F\bar{4}3m$ space group using the atomic positions of Li_2MgSi [11] as a starting model. Table 1 lists the results for both as-milled and thermally desorbed samples, as well as the corresponding DFT results obtained by optimizing the structure with VASP. Fig. 1 shows the experimental, calculated and difference intensity patterns. The pattern of the hydrogen cycled material has considerably sharper reflections due to the annealing effects of thermal absorption and desorption of hydrogen. The R_{wp} values for the as-milled and cycled material are 12.4% and 13.0%, respectively, indicating a reasonably good fit of the model to the observed PXRD pattern. The Li ions occupy the 1b, 3c and 4e Wyckoff positions, Mg ions are on the 1a and 3d sites, and Pt atoms are located on 4e positions. The Li ions at the 1b and 3c sites and both Mg ions are tetrahedrally coordinated by Pt atoms, while the Li ion on the 4e site resides in an irregular cage. The single crystallographically unique Pt site is coordinated with 4 Li and 4 Mg ions in a cuboidal bonding environment. Due to the weak X-ray scattering of Li the location of the 4e site was not refined from the starting

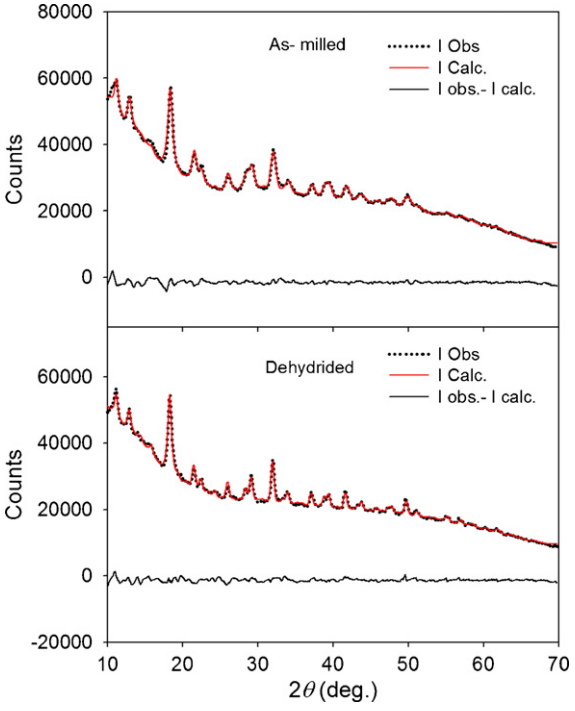

Fig. 1. Powder X-ray Rietveld refinement plot for as-milled Li_2MgPt (upper panel) and Li_2MgPt after one hydrogen absorption and desorption cycle (lower panel).

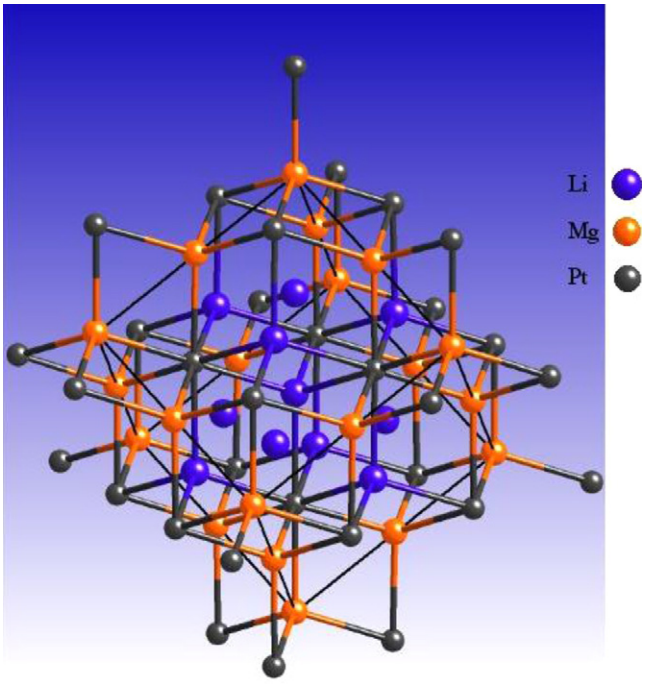

Fig. 2. Crystal structure of Li_2MgPt. The black line indicates the unit cell. All Mg and Li atoms with the exception of the 4e Li sites are tetrahedrally coordinated with Pt. Pt is in an eightfold coordinated cuboidal environment of 4 Mg and 4 Li atoms. The 4e Li atom resides in a cage and is only loosely associated with Mg.

position obtained from Li_2MgSi. Fig. 2 is a diagram of the Li_2MgPt crystal structure.

Using the electronic total energies E obtained from VASP computations we can estimate the formation enthalpy (i. e., the calculated standard enthalpy of formation at zero temperature in the absence of zero point energy contributions) of Li_2MgPt:

$$\Delta H(Li_2MgPt\ P\bar{4}3m) \equiv E(Li_2MgPt\ P\bar{4}3m) - 2\,E_{el}(Li) - E_{el}(Mg) - E_{el}(Pt)$$

$$= -222\ \text{kJ/mole}\ Li_2MgPt. \quad (1)$$

This value is properly lower than $\Delta H(Li_2MgPt\ F\bar{4}3m) = -220$ kJ/mole Li_2MgPt and $\Delta H(Li_2MgPt\ Fm\bar{3}m) = -193$ kJ/mole Li_2MgPt obtained for the two hypothetical template structures in our DFT investigation.

4. Hydriding properties

Approximately 1 mass% hydrogen, corresponding to slightly less than two H atoms per Li_2MgPt formula unit, was absorbed by an as-milled sample hydrided according to the schedule described in Section. 2. The PXRD pattern of the product material indexed to the $MgPtC_{0.06}H_{0.32}$ phase (tetragonal, $P4/mmm$, $a = 2.957$ Å and $c = 3.509$ Å) synthesized by Aleandri et al. [12] via thermal decomposition of Mg and Pt salts in solution.

Since no carbon was introduced in our experiments, we investigated the claim made by Aleandri et al. [12] that adventitious carbon is necessary to stabilize $MgPtC_{0.06}H_{0.32}$. Elemental Mg and Pt alone were combined in a 1.1:1 Mg:Pt ratio, cold pressed into a pellet, and sealed under Ar in a stainless steel tube. The charge was heated to 800 °C over 4 h and held at that temperature for an additional 48 h. The sample was air quenched, yielding a sintered pellet. The PXRD pattern of the heat treated sample could be indexed to that of $MgPtC_{0.06}H_{0.32}$ with only slightly different lattice constants: $a = 2.945$ Å (0.3% difference) and $c = 3.495$ Å (0.5% difference). Assuming that the MgPt structure is described as in Ref. [12]

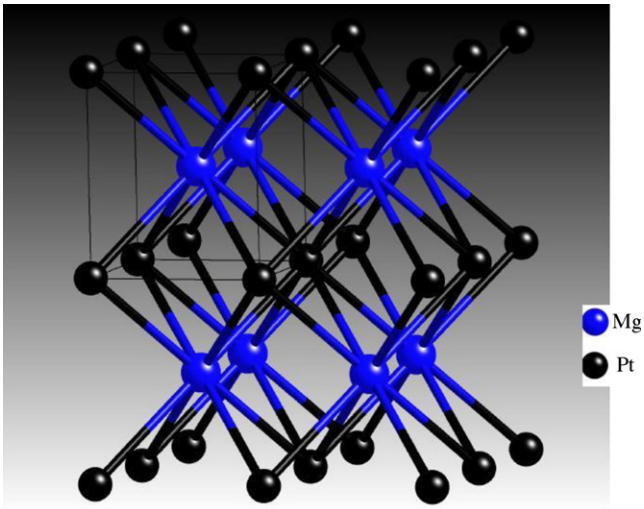

Fig. 3. Crystal structure of MgPt, based on the $MgPtC_{0.06}H_{0.32}$ structure from Ref. [12] with C and H neglected. Comparison of the powder pattern for the hydrided product of Li_2MgPt and the pattern calculated for this structure demonstrated that MgPt is one of the products of the hydriding reaction of Li_2MgPt.

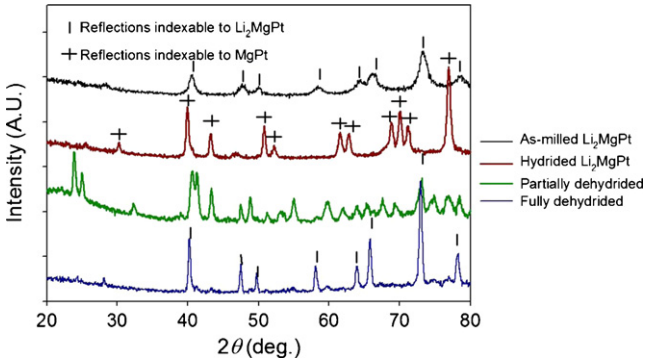

Fig. 4. Powder X-ray diffraction patterns for four hydrogen sorption stages of the Li_2MgPt system prepared with 2:1.5:1 Li:Mg:Pt starting atomic ratios: as-milled, hydrided, partially dehydrided to an unidentified phase, and fully dehydrided back to Li_2MgPt. The vertical hash marks indicate reflections indexable to the primitive cubic parent phase, and the plus marks signify reflections belonging to the $MgPtC_{0.06}H_{0.32}$ phase from Ref. [12].

with the exclusion of carbon and hydrogen, optimization with VASP yields $a = 3.008$ Å and $c = 3.529$ Å, in reasonable agreement with our measurements. Given these findings we conclude that neither carbon nor hydrogen is necessary to stabilize MgPt and that it is a new member of the Mg–Pt binary phase diagram. Of note is the difference in the calculated and experimental lattice parameters. This could be due to the fact that the binary MgPt has a homogeneity range such that the sample may have Mg vacancies or mixed occupancy with Pt (though Pt can be refined to full occupancy) leading to the observed contraction of the lattice parameters with respect to those calculated for a fully occupied, crystallographicaly ordered phase. The calculated densities of states indicate that MgPt and Li_2MgPt are both metals. The crystal structure of the heretofore unknown phase MgPt is shown in Fig. 3. Pt atoms occupy the 1a Wyckoff position and Mg resides on the 1d site. The measured density (by pycnometry) is 12.3 g/cm^3, consistent with the measured X-ray density of 12.1 g/cm^3. This value, however, is approximately a factor of two larger than the measured density of the hydrided Li_2MgPt sample.

Given the uptake of ~2 hydrogen atoms and our observation that only lines for a true MgPt binary appear in the powder pattern of the hydrided product, we infer that hydriding of Li_2MgPt proceeds according to the reaction

$$Li_2MgPt + H_2 \rightarrow 2LiH + MgPt. \quad (2)$$

No LiH reflections were observed in the powder pattern of the hydrided materials, but due to the much stronger X-ray scattering power of Mg and Pt, LiH is unlikely to be seen even if present to greater than 65 mol%. Additionally, pycnometry measurements of the hydrided samples yielded a density of 6.1 g/cm^3, which is consistent with the density predicted for a mixture of 2 molar equivalents of LiH and 1 of MgPt. As with the Li_2MgSi and Li_2MgIr representatives of this structure type, Li_2MgPt decomposes on exposure to hydrogen. Li_2MgSi decomposes to Mg_2Si, LiH, and elemental Si [11], while Li_2MgIr forms LiH and the complex hydride $LiMgIrH_6$ [3]. These findings point to intrinsic instability of the structure under the conditions of thermal hydriding.

In our exploratory DFT study we investigated the possible formation of quaternary Li_2MgPtH_n hydrides by calculating ΔH for eight distinct template structures. For the Li_2MgPtH_2 stoichiometry we obtained enthalpies ranging from −64 to −103 kJ/mole H_2 for three of the Li_2MgPtH_2 models. All of these values, however, are less negative (higher in energy) than the enthalpy of reaction $\Delta H_R = -120$ kJ/mole H_2 calculated for Eq. (2). That is, all the hypothetical quaternary hydride structures, despite featuring negative formation enthalpies, are thermodynamically unstable with respect to decomposition to LiH and MgPt, in accord with our experimental results. This emphasizes the important point that theoretical model calculations, however encouraging, can only be considered as guides for the identification of new materials. Complementary experimental investigation is crucial.

To demonstrate conclusively that hydriding of Li_2MgPt proceeds by reaction (2), a sample of MgPt was combined in a 1:2 ratio with LiH powder by milling for 1 h. The milled powder had a measured density consistent with the density of the hydriding reaction product (6.1 g/cm^3), as well as an identical PXRD pattern. As before, LiH was not observed in the PXRD diagram. The milled powder was then dehydrided thermally in the hTGA, and it lost mass consistent with two hydrogen equivalents. Evolved gas analysis revealed only H_2 in the mass spectrum. PXRD of the reaction product demonstrated that the cubic parent Li_2MgPt forms by this route, further supporting reaction (2). Importantly, in both the dehydriding reaction of the milled MgPt and LiH powders and the hydriding product of Li_2MgPt, the onset of hydrogen desorption occurs at the same temperature, ~350 °C, approximately 350 °C below the dehydriding temperature of pure LiH (~700 °C), indicating that MgPt plays a destabilizing role for LiH. This is mostly likely due to the negative formation enthalpy of the cubic parent [cf. Eq. (1)] which acts as a driving force for the dissociation of both LiH and MgPt. This behavior is similar to that of the $LiBH_4/MgH_2$ system, which liberates hydrogen at a much lower temperature than either of the two components would in isolation due to the thermodynamic driving force provided by the formation of MgB_2 [13].

During the investigation of hydrogen sorption in this system it was observed that depending on the Mg content of the initial milling reaction different products were obtained upon thermal desorption of the MgPt + 2LiH mixture. One is the cubic parent Li_2MgPt, which was recovered in high purity from samples that originated from milled materials with a larger excess of Mg in the starting composition. For samples whose original nominal compositions are closer to the Li_2MgPt stoichiometry, on the other hand, the powder pattern of the dehydrided product indicates another phase (or phases) whose structure is unknown. Hydrogen adsorption experiments performed on a series of samples with varying levels of excess Mg found all samples to take up hydrogen, and the hydride products all had powder patterns whose reflections

could be indexed to MgPt with no other major phases observed. Upon thermal desorption samples with excess Mg lost more weight, indicating a more fully dehydrided product, and generally yielded Li_2MgPt either as a single phase or a dominant phase in a mixture with an unidentified intermediate phase (or phases). As the amount of excess Mg was decreased the amount of the unidentified intermediate phase increased to a point that a stoichiometric sample gave no detectable reflections of Li_2MgPt after thermal desorption from the hydrided state. It was also found that the purity of the milled parent phase increased with increasing excess Mg. These findings suggest that Mg loss during the various stages of reaction ultimately leads to the destabilization of the cubic parent and favors the formation of the intermediate phase (or phases). Indeed, samples with a large excess of Mg in the original nominal composition tend to form the intermediate phase as the number of cycles of hydrogen absorption and desorption increases. The intermediate phase neither releases nor absorbs as much hydrogen as cycling back to the parent phase alone, and so the hydrogen storage capacity gradually deteriorates. Fig. 4 shows the PXRD patterns for the reaction products of a sample with initial Li:Mg:Pt atomic ratios of 2:1.5:1 at various stages: as-milled, hydrided, partially desorbed, and fully desorbed to the cubic parent. Nascent impurity lines are visible in the pattern for the fully dehydrided sample. This materials system does not reversibly cycle hydrogen.

Acknowledgements

It is a pleasure to thank Richard L. Speer for powder X-ray diffraction and Nick Irish for ICPMS elemental analysis. Mercouri G. Kanatzidis and the diffraction facility at Northwestern University for use of the STOE X-ray diffractometer are also gratefully acknowledged.

References

[1] P. Villars, L.D. Calvert, Pearson's Handbook of Crystallographic Data for Intermetallic Phases, second ed., ASM International, Materials Park, OH, 1991.
[2] W. Kohn, L. Sham, Phys. Rev. 140 (1965) A1133.
[3] J.R. Salvador, J.F. Herbst, M.S. Meyer, J. Alloys Compd., accepted for publication.
[4] "FULLPROF: A Program for Rietveld Refinement and Pattern Matching Analysis", by J. Rodríguez-Carvajal, at the Satellite Meeting on Powder Diffraction of the XV IUCr Congress, 127 (1990).
[5] G. Kresse, J. Hafner, Phys. Rev. B 49 (1994) 14251.
[6] G. Kresse, J. Furthmüller, Comput. Mater. Sci. 6 (1996) 15.
[7] P.E. Blöchl, Phys. Rev. B 50 (1994) 17953.
[8] G. Kresse, D. Joubert, Phys. Rev. B 59 (1999) 1758.
[9] J.P. Perdew, Y. Wang, Phys. Rev. B 45 (1992) 13244.
[10] J.P. Perdew, J.A. Chevary, S.H. Vosko, K.A. Jackson, M.R. Pederson, D.J. Singh, C. Fiolhais, Phys. Rev. B 46 (1992) 6671.
[11] J.F. Herbst, M.S. Meyer, J. Alloys Compd. 492 (2010) 65.
[12] L. Aleandri, B. Bogdanović, U. Wilczok, D. Noreus, G. Block, Z. Phys. Chem. 185 (1994) S131.
[13] J.J. Vajo, S.L. Skeith, R. Mertens, J. Phys. Chem. B 109 (2005) 3719.